Available online www.jocpr.com

Journal of Chemical and Pharmaceutical Research, 2018, 10(4): 60-73

Research Article

ISSN : 0975-7384
CODEN(USA) : JCPRC5

Molecular Structure Impacts on Nonlinear Optical Activity of Novel Pyrimidinone Derivative

U Uma Devi[1], A Dhandapani[2], D Durgadevi[3] and S Manivarman[1*]

[1]PG and Research Department of Chemistry, Government Arts College, C Mutlur, Chidambaram 608102, Tamil Nadu, India
[2]CK College of Engineering and Technology, Cuddalore 607 003, Tamil Nadu, India
[3]Aries Arts and Science College, Vadalur-607 303, Tamil Nadu, India

---

ABSTRACT

Highly functionalized dihydropyrimidine has been synthesised by biginelli one pot multi component condensation reaction. Spectral analysis of the synthesized compound has been proposed by UV, FT-IR and NMR spectral analysis. Theoretical calculations were performed by DFT/B3LYP/6-311++G(d,p) level of theory. The optimized molecular structure and fundamental harmonic vibrations were compared with experimental data. The chromophores which are responsible for the electronic transition are determined by frontier molecular orbital analysis. The stabilization energy of the studied molecule during electron delocalisation and molecular interactions are calculated by second order perturbation analysis. From the results of NLO studies, the title compound is a good candidate for nonlinear optics with highest hyperpolarizability value.

Keywords: Pyrimidinone; DFT; HOMO-LUMO; Donor-acceptor interactions

---

INTRODUCTION

Nitrogen containing heterocyclic compounds has shown phenomenal pharmacological activities. In particular, pyrimidine and its derivatives have implausible biological and medicinal relevance and are used as anticancer, antiviral, anti-inflammatory, anti-HIV, anti-tumour and anti-bacterial agents [1-9]. In addition, pyrimidine based molecules also attracted for their valuable optical and physical properties. Organic molecules bearing pyrimidine nucleus have exhibit fluorescent radiometric chemosensory, luminescent materials and inhibition of corrosion of metal surface [10-12]. Nowadays, computational chemistry becomes a very useful field in interpretation, understanding and simulation of experimental data. Theoretical calculations are widely used for the determination of the electronic properties and elucidating the structure-activity relationships of synthesized and natural organic compounds [13,14].

Based on the incredible importance of the pyrimidines, we are planned to synthesize a pyrimidine derivative, ethyl-2-(chloromethyl)-8-methoxy-4-oxo-3,4,5,6-tetrahydro-2H-2,6-methanobenzo(g)(1,3,5)oxadiazocine-11-carboxylate(ECMC).The synthesized molecule is subjected for combinatorial study. The molecular structure has been studied using experimental data and also with theoretical predictions. In addition to that, some electrochemical properties are also studied to know about the impact of molecular properties on nonlinear optical property.

EXPERIMENTAL SECTION

Synthesis of ethyl-2-(chloromethyl)-9-methoxy-4-oxo-3,4,5,6-tetrahydro-2H-2,6-methanobenzo(g)(1,3,5)oxadiazocine-11-carboxylate

2-Hydroxy-5-methoxybenzaldehyde (0.76 g, 5 mmol) and urea (0.9 g, 15 mmol) was added to an ethanolic solution of ethyl acetoacetate (0.65 ml, 5 mmol). To the mixture $CeCl_3.7H_2O$ (0.465 g, 25%) was added and stirred well. After the addition was complete, the reaction mixture was refluxed at 90°C. After reaction completion, the mixture being cooled to room temperature and poured on to crushed ice. The content is stirred for 5-10 mins. The solid was separated and filtered under suction, then recrystallized from DMSO (Scheme 1).

Melting point = 195°C; Yield = 93%.

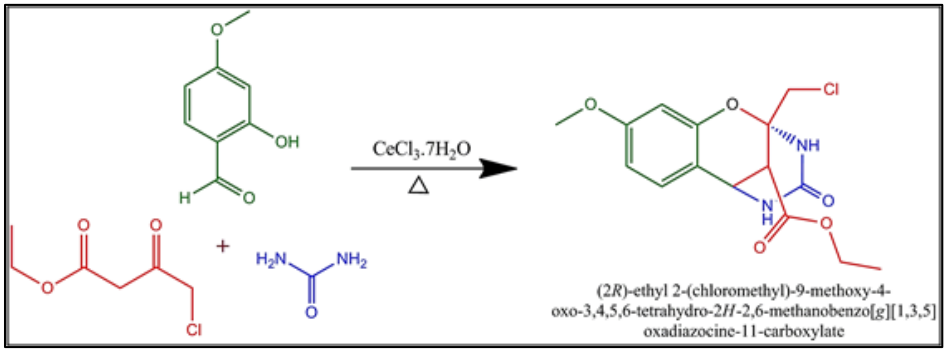

Scheme 1: Synthesis of ethyl-2-(chloromethyl)-9-methoxy-4-oxo-3,4,5,6-tetrahydro-2H-2,6- methanobenzo(g)(1,3,5) oxadiazocine-11-carboxylate

Structural Determination

The newly synthesized oxygen bridged pyrimidinone derivative ECMC molecular structure was elucidated using FT-IR, FT-Raman and NMR spectral analysis. The ^1H and ^{13}C-NMR spectra of ECMC are shown in Figures 1,2.

The spectral values are given below.

^1H NMR (400 MHz, $DMSOd_6$): δ = 6.74-6.84 (m, ArH), 7.73 (s, NH), 7.46 (s, NH), 1.21-1.26 (t, 2H, CH_3), 3.70 (s, 1H, CH_3), 4.31 (d,1H); ^{13}C-NMR (100 MHz, $DMSOd_6$): δ = 167.8, 154.1, 113.1-153.3, 83.8, 60.9, 55.3, 47.6, 13.9.IR (KBr) νcm^{-1}; 3338, 3214cm^{-1} (NH), 3080 cm^{-1} (Ar-CH), 2965 cm^{-1}(C_{10}-H_{32}), 1740 cm^{-1} (C=O), 1588cm^{-1} (C=C).

Computational Details

In the present study, Gaussian 03 program is used to compute the theoretical calculations of ECMC by using DFT/B3LYP gradient with 6-31G (d,p) basis set. The vibrational modes of the synthesised compound were assigned on the basis of PED analysis using VEDA4 program [15]. The theoretical wavenumbers were scaled down uniformly by a scale factor of 0.9608 for close proximity with experimental results.

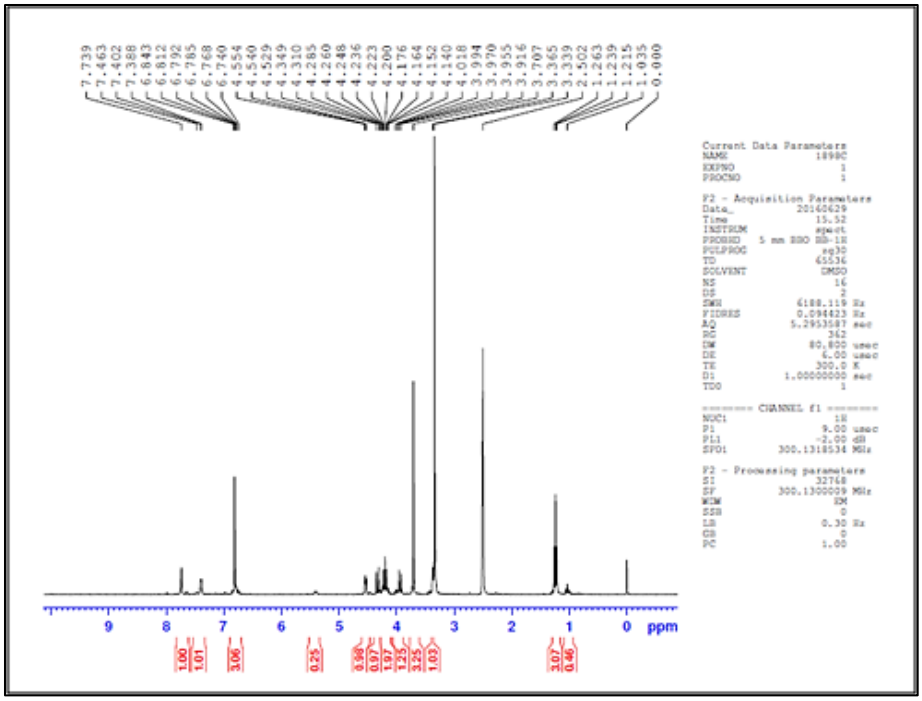

Figure 1: ^{1}H-NMR Spectrum of ECMC

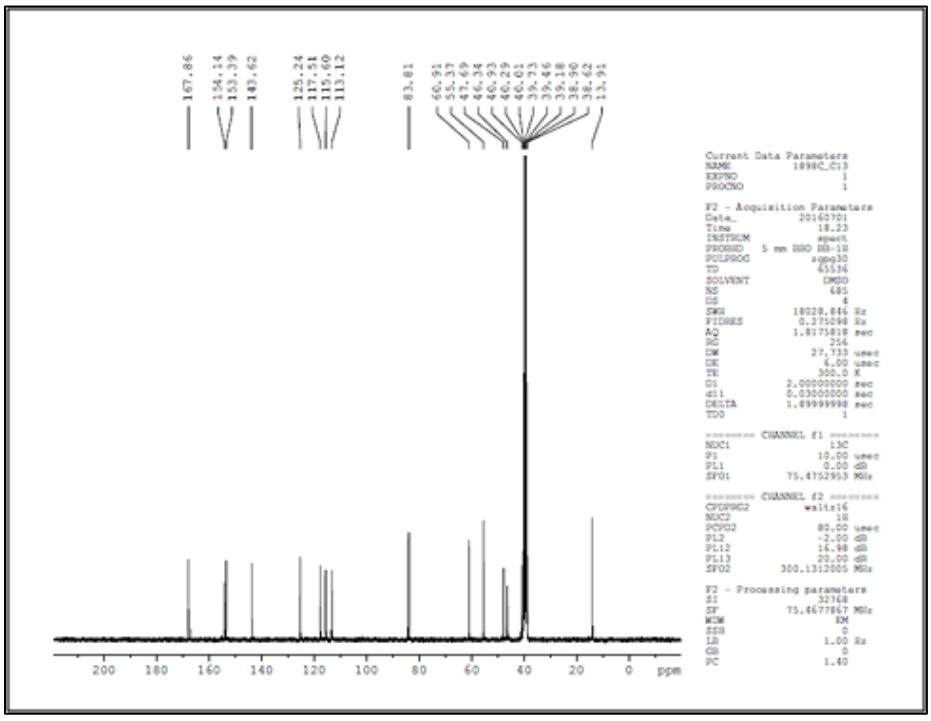

Figure 2: ^{13}C-NMR spectrum of ECMC

RESULTS AND DISCUSSION

Geometrical Structural Parameter

The optimized structural parameters such as bond length and bond angles of ECMC is calculated theoretically using DFT/B3LYP/6-311++G(d,p) level of theory. Table 1 consists of geometrical parameters of optimized structure of ECMC. The energy minimized optimized structure of ECMC with atom numbering is shown in Figure 3. There is no exact crystal data available for the title compound, hence, the calculated geometrical parameters are comparatively studied with the experimental crystal data obtained for analogous molecule of ethyl-(2S)-9-methoxy-2-methyl-4-oxo-3,4,5,6-tetrahydro-2H-2,6 methanobenzo(g)(1,3,5)oxadiazocine-11-carboxylate, reported by Dhandapani et al [16].

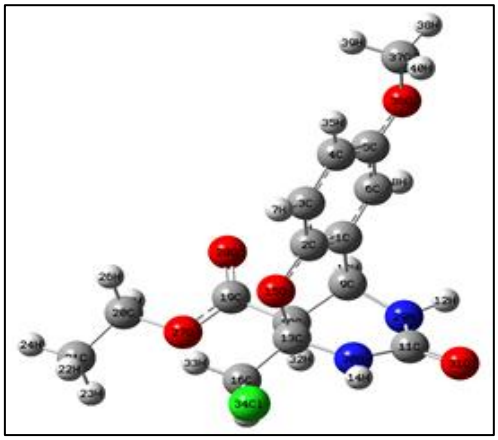

Figure 3: The optimized structure of ECMC

For the title compound, the C–C bond length in aromatic ring lies is in the range of 1.39-1.40 Å, while in pyrimidine ring, the C–C bond length values are slightly higher, because C_9, C_{10} and C_{13} atoms are sp^3 hybridized carbons and are attached with electronegative nitrogen atom. The carbonyl bond lengths are calculated as 1.22 and 1.21 Å. The C–O bond lengths are calculated in the range from 1.36-1.45 Å, which shows good agreement with literature values of C–O bond length.

Table 1: The geometrical parameters of ECMC

Bond length	(Å)	Bond length	(Å)	Bond angle	(°)
C1–C2	1.4	C21–H24	1.09	C13–C16–H33	110.39
C1–C6	1.39	O36–C37	1.41	C13–C16–Cl34	112.51
C1–C9	1.52	C37–H38	1.09	H17–C16–H33	110.32
C2–C3	1.39	C37–H39	1.09	H17–C16–Cl34	106.74
C2–O15	1.38	Bond angle	(°)	H33–C16–Cl34	106.64
C3–C4	1.39	C3–C2–O15	117.25	C10–C19–O27	111.58
C3–7H	1.08	C2–C3–C4	120.37	C10–C19–O28	124.61
C4–C5	1.4	C2–C3–H7	118.85	O27–C19–O28	123.69
C4–H35	1.08	C4–C3–H7	120.76	C21–C20–H25	112.23
C5–C6	1.39	C3–C4–C5	119.76	C21–C20–H26	112.37
C5–O36	1.36	C3–C4–H35	119.11	C21–C20–O27	107.58
C6–H8	1.08	C5–C4–H35	121.12	H25–C20–H26	107.64
C9–C10	1.53	C4–C5–C6	119.42	H25–C20–O27	108.34
C9–H18	1.09	C4–C5–O36	124.83	H26–C20–O27	108.54
C9–N29	1.46	C6–C5–O36	115.73	C20–C21–H22	111.2
C10–C13	1.55	C1–C6–C5	121.07	C20–C21–H23	111.06
C10–C19	1.52	C1–C6–H8	120.6	C20–C21–H24	109.58
C10–H32	1.09	C5–C6–H8	118.31	H22–C21–H23	108.47
C11–N29	1.38	C1–C9–C10	110.23	H22–C21–H24	108.15
C11–N30	1.39	C1–C9–H18	109.81	H23–C21–H24	108.26
C11–O31	1.22	C1–C9–N29	112.7	C19–O27–C20	115.81
H12–N29	1.01	C10–C9–H18	109.61	C9–N29–C11	118.81
C13–O15	1.43	C10–C9–N29	106.05	C9–N29–H12	117.21
C13–C16	1.53	H18–C9–N29	108.3	C11–N29–H12	111.72
C13–N30	1.44	C9–C10–C13	105.13	C11–N30–C13	128.06
H14–N30	1.01	C9–C10–C19	111.09	C11–N30–H14	113.43
C16–H17	1.08	C9–C10–H32	108.93	C13–N30–H14	116.85
C16–H33	1.08	C13–C10–C19	115.74	C5–O36–C37	118.05

C16–Cl34	1.81	C13–C10–H32	108.12	O36–C37–H38	106.04
C19–O27	1.34	C19–C10–H32	107.62	O36–C37–H39	111.71
C19–O28	1.21	N29–C11–N30	114.59	O36–C37–H40	111.72
C20–C21	1.51	N29–C11–O31	123.46	H38–C37–H39	109.12
C20–H25	1.09	N30–C11–O31	121.86	H38–C37–H40	109.12
C20–H26	1.09	C10–C13–O15	108.88	H39–C37–H40	109.01
C20–O27	1.45	C10–C13–C16	113.29	C13–C16–H17	110.09
C21–H22	1.09	C10–C13–N30	107.13	C2–C1–C6	118.96
C21–H23	1.09	O15–C13–C16	104.97	C2–C1–C9	119.57
C37–H40	1.09	O15–C13–N30	112.85	C6–C1–C9	121.43
		C16–C13–N30	109.81	C1–C2–C3	120.38
		C2–O15–C13	116.65	C1–C2–O15	122.31

The N–H and C–H bond length values are calculated as 1.01 and 1.08-1.09 Å respectively. The C–N bond lengths are calculated as 1.39, 1.38, 1.44 and 1.46 Å, in which bond length of C_9–N_{29} and C_{13}–N_{30} are slightly higher. This is due to nitrogen atoms attached with sp^3 hybridised carbon atom.

Generally sp^2 hybridised carbon atoms have bond angle around ~120°. In the present study, bond angle of sp^2 hybridized carbon atoms are in the range of 117-122°, in which C_5, C_{11} and C_{19} carbon atoms somewhat deviated from their normal bond angle, this is due to these atoms attached with electronegative atoms such as nitrogen and oxygen. Similarly, sp^3 hybridised C_{13} and C_{37} atoms also deviated to some extent and bond angle of other sp^3 carbon atoms are in the range of 107-111°.

Intramolecular Stabilization Analysis

A detailed description of molecular interaction of the ECMC compound can be explained by NBO analysis. It is used to find the interaction between the bond orbitals, electron delocalization, intramolecular charge transfer (ICT) and identification of hydrogen bonding. In this analysis, the electron wave functions are interpreted in terms of bonding and antibonding orbitals, these orbitals corresponds to delocalization of electron density between donor acceptor interactions. The delocalization effects (or donor acceptor charge transfers) can be estimated from the off-diagonal elements of the Fock matrix in the NBO basis [17-19]. The various donor-acceptor interactions of ECMC are listed in Table 2.

The molecular interaction of the title compound mainly occur from the σ occupied orbital to the σ* unoccupied orbital. The energy interactions from bonding orbital σ(N_{29}–H_{12}) to anti bonding σ*(C_9– C_{10}, C_{11}– N_{30}) resulting the stabilization energies of 8.66 and 20.04 KJ/mol with occupancy of 0.0236 and 0.0827e, respectively. Some other strong σ– σ* interactions of the title molecule are σC_1–C_2→ σ*C_1–C_6, C_2–C_3, σC_1–C_6→ σ*C_1–C_2, C_2–O_{15}, σ C_2–C_3→ σ*C_1–C_2, σ C_3–C_4→ σ*C_1–O_{36}, , σ N_{30}–H_{14}→ σ*C_{11}–N_{29}, σC_{21}–H_{24}→ σ*C_{20}–O_{27} with the stabilization energies of 15.73, 17.45, 17.87, 18.33, 19.04, 19.83, 18.45 and 19.54 KJ/mol respectively. From the results, it is clear that the strong interaction of σ(N_{29}–H_{12}) → σ*(C_9–C_{10}, C_{11}– N_{30}) make the title molecule stabilized.

Table 2: Second order perturbation theory analysis of Fock matrix in NBO basis for ECMC

Type	Donor (i)	ED/e	Acceptor (j)	ED/e	[a]E(2) (kJ/mol)	[b]E(j)−E(i) a.u	[c]F(i, j) a.u
π -π*	C1 - C6	1.709	C2 - C3	0.382	81.3	0.28	0.06
			C4 - C5	0.4043	83.05	0.28	0.06
			C9 - N29	0.0359	21.67	0.59	0.05
σ -σ*	C1 - C9	1.9708	C1 - C2	0.0344	7.87	1.19	0.04
			C1 - C6	0.0187	10.5	1.22	0.05
			C5 - C6	0.0207	9	1.2	0.04
			C10 - H32	0.0159	6.61	1.06	0.03
σ -σ*	C2 - C3	1.9748	C1 - C2	0.0344	19.04	1.27	0.06
			C1 - C9	0.0402	13.22	1.1	0.05
			C3 - C4	0.0123	10.25	1.29	0.05
			C3 - H7	0.0117	5.31	1.18	0.03
π -π*	C2 - C3	1.6641	C1 - C6	0.3738	87.19	0.29	0.07
			C4 - C5	0.4043	77.19	0.28	0.06
σ -σ*	C4 - C5	1.9804	C3 - C4	0.0123	11	1.29	0.05
			C3 - H7	0.0117	9	1.18	0.04
			C4 - H35	0.0124	5.44	1.18	0.03
π -π*	C4 - C5	1.6591	C1 - C6	0.3738	77.95	0.29	0.06
			C2 - C3	0.382	87.07	0.29	0.07
			C13 - N30	0.0559	6.9	1.02	0.03
			C20 - O27	0.0337	15.31	0.9	0.05
n -σ*	O15	1.959	C1 - C2	0.0344	26.94	1.12	0.07
			C10 - C13	0.048	10.92	0.86	0.04

			C13 - C16	0.0412	5.23	0.88	0.03
n -π*	O15	1.8587	C2 - C 3	0.382	94.43	0.35	0.08
			C10 - C13	0.048	16.65	0.63	0.04
			C13 - N30	0.0559	43.6	0.67	0.07
n -σ*	O27	1.9614	C19 - O28	0.0213	33.35	1.17	0.08
n -π*	O27	1.7897	C19 - O28	0.2151	207.44	0.33	0.11
			C20 - H25	0.019	16.78	0.78	0.05
			C20 - H26	0.0188	16.4	0.79	0.05
n -σ*	O28	1.9754	C10 - C19	0.0676	10.75	1.06	0.04
			C19 - O27	0.1004	5.82	1.06	0.03
n -π*	N29	1.7862	C1 - C6	0.3738	4.64	0.32	0.01
			C1 - C9	0.0402	33.35	0.68	0.06
n -π*	O36	1.8468	C4 - C5	0.4043	124.6	0.34	0.09
			C37 - H39	0.0203	23.35	0.74	0.05
			C37 - H40	0.0203	23.35	0.74	0.05

[a]E(2) means energy of hyper conjugative interaction (stabilization energy).
[b]F(i,j) is the fork matrix element between i and j NBO orbitals.
[c]Energy difference between donor (i) and acceptor (j) NBO orbitals.

In the present study, the σ-σ* interaction have minimum delocalization energy then π– π* interaction. Hence, the σ bonds have higher electron density than the π bonds. For the title compound, π electron delocalisation takes place around phenyl ring of the title compound. The maximum stabilization energies 83.05, 87.16 and 87.07 KJ/mol are due to π electron delocalisation of C_1–C_6, C_2–C_3, C_4–C_5 bonds distributed energies to their respective aniti bond π* orbitals with occupancy of 0.4043, 0.3778 and 0.3820 e, respectively.
Similarly, the maximum stabilization energy resulted due to π electron delocalisation non-bonding electrons to anti bonding orbitals. The stabilization energy of 207.44 and 124.6 KJ/mol due to transfer of energy from nonbonding electrons of O_{27} and O_{36} distributed to anti bonding orbitals of π*C_{19}–O_{28} and π*C_4–C_5. The energetic stabilization in ECMC reveals the charge transfer from lone pair of oxygen to respective acceptor bonds.

Molecular Electrostatic Surface Potential (MESP)
The total charge distribution of the molecule can be determined by molecular electrostatic potential surface. MEP is a useful tool to interpret hydrogen bonding and it correlates with dipole moments, electro negativity and chemical reactivity of the molecules. The potential increases on MEPS in the order, red<orange<yellow<green<blue [20]. From the Figure 4, it has been seen that, the negative potential region is localized at O_{15}, O_{17}, O_{28}, O_{31}, O_{36} atoms of the ECMC compound. The most electropositive potential spread over N_{29} and N_{30} atoms, which is preferrable site for nucleophilic attack.

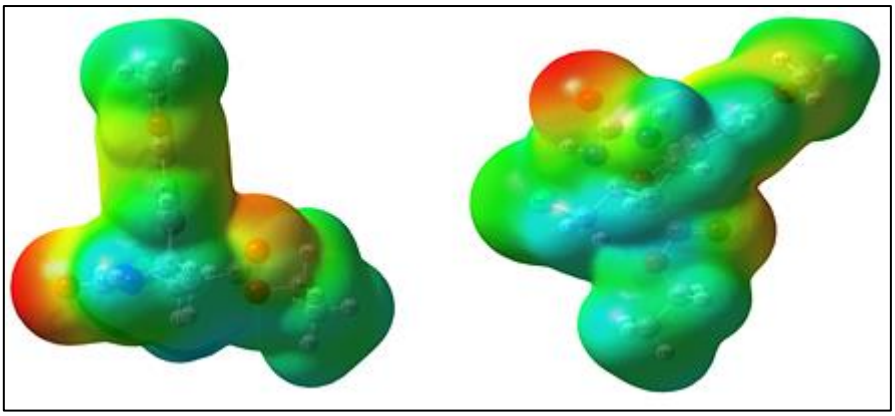

Figure 4: The molecular electrostatic potential surface of ECMC

Electronic Absorption Studies
In order to analyse the electronic transition of the title compound, UV spectrum was recorded within the range of 200-400 nm using ethanol as a solvent and representative spectrum is shown in Figure 5. From this observation, the strong band at 250 nm exhibit the π-π* transition takes place within the ECMC compound. Theoretically, the electronic absorption was calculated by time dependent density functional theory (TD-DFT). The computed electronic values, such as absorption wavelength (λ_{max}), excitation energies (E), oscillator strength (f) and assignments of electronic transitions for title compound are given in Table 3.
The theoretical absorption band at 263 nm shows good agreement with experimental absorption band with slight red-shift. This is due to attractive polarisation forces between the solvent and the molecule, which lower the

energy levels of both the excited and unexcited states. The calculated and recorded UV-Vis spectrum of the title compound is shown in Figure 5.

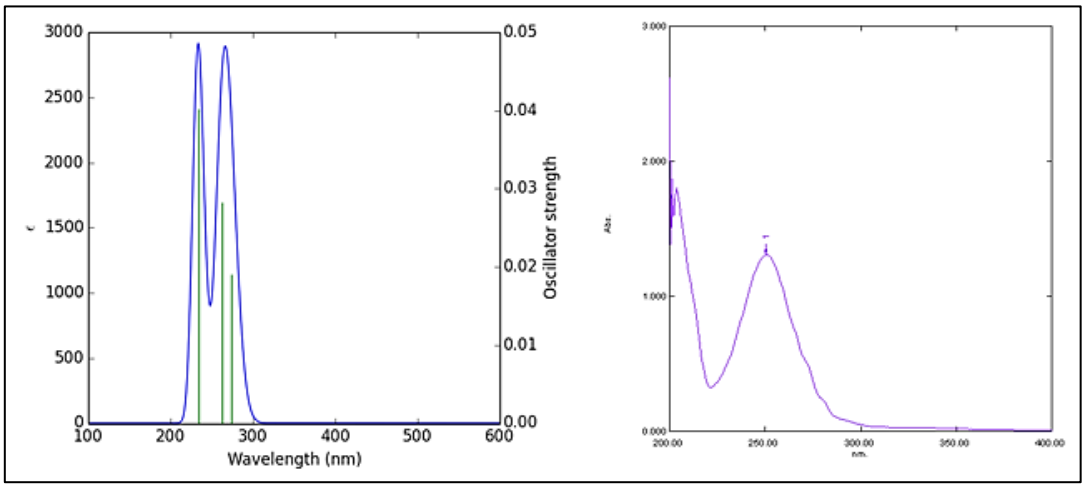

Figure 5: The theoretical and experimental UV spectra of ECMC

Table 3: The excitation energies and oscillator strength of ECMC

TD-DFT/B3LYP/6-31G(d,p)					Experimental λmax(nm)
Orbitals	**CI expansion coefficient**	**Energy gap**	**Oscillator strength (*f*)**	**Calculated Wavelength λmax(nm)**	
Excited State 1:	Singlet-A				
89 → 90	0.68003	4.5233	0.019	274.1	
89 → 91	-0.14421				
Excited State 2:	Singlet-A				
88 → 92	-0.11458	4.7113	0.0282	263.16	250.5
89 → 90	0.11191				
89 → 91	0.67117				
Excited State 3:	Singlet-A				
89 → 92	0.65398	5.2948	0.0402	234.16	
89 → 93	0.20463				

FMO Analysis

Frontier orbitals of a molecule are simply considered as the highest occupied molecular orbital (HOMO) and lowest unoccupied molecular orbital (LUMO). The regions of highest electron density (HOMO) represent the electrophilic-attacking sites, whereas the LUMO reflects the nucleophilic-attacked sites [21,22]. These molecular orbitals are considered to assess the kinetic characteristics of reactants and reactions. These are likely to be the major initial interactions as reactants approach since, at distances somewhat greater than typical bond lengths, the greatest orbital overlap is between frontier molecular orbitals. They are used to find frontier electron density for predicting the most reactive position in π-electron systems. The chemical stability of a molecule can be characterized by the gap between HOMO and LUMO. A small gap indicates the significant degree of intermolecular charge transfer from electron-donor groups to the efficient electron-accepter groups through π-conjugated path [23].

The HOMO-LUMO amplitude of the ECMC compound is shown in Figure 6. It is noted that HOMO is confined over the pyrimidine moiety and LUMO is located over phenyl ring. The HOMO-LUMO energy gap of the title molecule is 4.4288 eV. The FMO orbitals are used to calculate the global reactivity descriptors, such as ionization energy (I), electron affinity (A), Global hardness (η), chemical potential (μ) and global electrophilicityindex (ω). These values are presented in Table 4. From that, it can be noted that, the energy gap of the investigated molecule is small and the value of chemical potential is negative hence ECMC compound is more stable and polarizable.

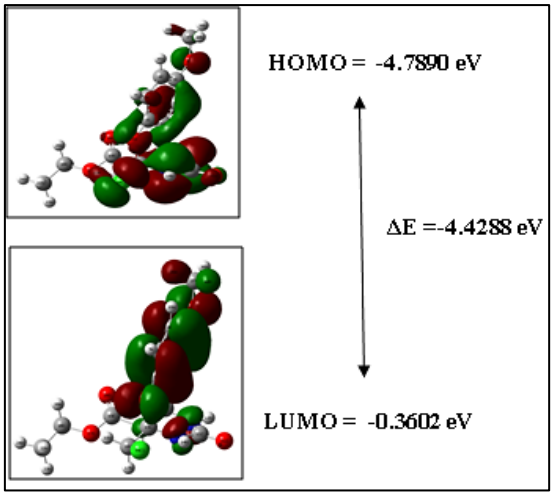

Figure 6: The frontier molecular orbitals of ECMC

Table 4: Global reactivity descriptors of ECMC

Global reactivity descriptors	Values (eV)
HOMO	-4.789
LUMO	-0.3602
energy gap (ΔE) = HOMO–LUMO	-4.4288
ionization energy I = $-E_{HOMO}$	4.789
electron affinity A =	0.3602
Global hardness (η)= 1/ 2(E_{LUMO}– E_{HOMO})	2.2144
Global softness (s) = S = 1/ 2η	0.2257
Electronegativity (χ) = –1/ 2(E_{LUMO}+ E_{HOMO})	2.5746
Chemical potential (μ) = - χ	-2.5746
global electrophilicity index (Ψ) = μ^2/ 2η	1.4966

Nonlinear Optical Property

Nonlinear optical material have an enormous role to use in a wide range of the areas from lasers to optical switches, i.e, communication, signal processing and optical sensing [24-26], hence investigation of NLO properties of a compound getting important in scientific aspect. In this context, the static dipole moment (μ), polarizability (α) and the first-order hyperpolarizability (β) of the title compound have been computed at B3LYP level of the theory based on the finite- field approaches [27-29] to predict the NLO properties, presented in the Table 5.

The static dipole moment is predicted as 1.9263 D and the anisotropy of the polarizability (α) are found out to be 3.9406×10^{-30}esu. The first-order hyperpolarizability (β) of the title compound is calculated as $3.4097\text{x}10^{-30}$esu. As well known, urea is the prototype compound to elucidate the NLO properties of the molecular systems. From the results obtained from the NLO analysis, we can suggested the title compound can be good non-linear optic compound because the first order hyperpolarizability of title compound is around 9 times greater than those of the urea ($\beta=0.3728\text{x}10^{-30}$esu). Hence the investigated compound is a good candidate of non-linear optics.

Table 5: Non-linear optical properties of ECMC

Parameters	Dipole Moment	Parameters	Hyper polarizability
μ_x	0.3669	β_{xxx}	310.5
μ_y	-1.8786	β_{xxy}	2.21
μ_z	0.2164	β_{xyy}	60.61
μ	1.9263Debye	β_{yyy}	-154.58
Polarizability (α_0)	$\text{x}10^{-30}$esu	β_{xxz}	-14.51
α_{xx}	232.36	β_{xyz}	26.81
α_{xy}	15.26	β_{yyz}	97.18
α_{yy}	166.74	β_{xzz}	-25.83
α_{xz}	3.88	β_{yzz}	-22.16
α_{yz}	2.1	β_{zzz}	-4.62
α_{zz}	171.11	β_0	$3.4097\text{x}10^{-30}$esu
α	3.9406×10^{-30}esu		

*Reference value for urea μ=1.3732 Debye, $\beta_0=0.3728\text{x}10^{-30}$esu.

Assignment of Fundamental Bands

The vibrational analysis of ECMC was performed on the basis of the characteristic vibrations of methyl, carbonyl, thiocarbonyl and methine. The molecule under consideration belongs to the C_1 point group. In order to obtain the spectroscopic signature of the investigated molecule, frequency calculation analysis has been performed by DFT method using B3LYP/6-311++G(d,p) level of theory. The computed harmonic wavenumbers and their intensities of FT-IR and FT-Raman corresponding to the different normal modes are used for identifying the vibrational modes unambiguously. The calculated wavenumbers are compared with the experimental FT-IR and FT-Raman bands are summarised in Table 6 along with their PED contribution, intensities and force constants. The recorded FT-IR and FT-Raman spectrums are shown in Figures 7,8.

N-H and C–N Vibrations

For hetero aromatic compounds, the N–H stretching vibrations appeared in the region of 3500-3000 cm^{-1}[30-32]. In this study, N–H stretching vibration calculated at 3484 and 3482 cm^{-1}. This vibration experimentally observed at 3214, 3213 cm^{-1} in FT-IR spectrum and 3338 cm^{-1} in FT-Raman spectrum.

The C–N stretching vibrations are normally occurs in the region of 1400-1200 cm^{-1}[32]. The C–N stretching vibration of the title compound is calculated at 1397, 1363, 1066 and 934 cm^{-1}. These vibrations experimentally observed at 1373 cm^{-1} in FT-IR spectrum and 937 cm^{-1} in FT-Raman spectrum. The deformation vibration β_{NCN} observed at 648 cm^{-1} in FT-Raman spectrum, which is coincide well with theoretical wavenumber 640 cm^{-1}.

C–H Vibrations

The C–H stretching vibrations of aromatic compounds containing hetero atoms, commonly exhibit multiple weak bands in the region of 3100-3000 cm^{-1}[33]. In the present study, the band observed at 3080 cm^{-1} in FT-IR spectrum and 3060 cm^{-1} in FT-Raman spectrum are assigned to C–H stretching vibration of aromatic ring. These vibrations show good correlation with theoretical wavenumber at 3088 and 3072 cm^{-1}. The aromatic C–H in-plane-bending and out-of-plane bending vibrations observed at 1300-1000 cm^{-1} and 900-690 cm^{-1}respectively [34-37]. The computed wavenumbers at 1135 and 1138 cm^{-1} are assigned to in-plane-bending vibrations of C–H bond. The out-of-plane bending vibrations theoretically observed at 900 and 860 cm^{-1}. The aliphatic C–H stretching vibration appeared at 2965 cm^{-1} in FT-IR spectrum and this is supported by the theoretical wavenumber at 2967 cm^{-1}.

Methyl group Vibrations

Generally, the C-H stretching vibrations of methyl group are usually observed in lower wavenumber region than Aromatic C–H stretching. The aliphatic C–H stretching vibrations are normally observed in the region of 3000-2800cm^{-1}[37]. The asymmetric and symmetric stretching vibrations of methyl group are observed around 2980 and 2870 cm^{-1} respectively [38-41]. The title compound has three methyl groups, their asymmetric vibrations observed at 2936 cm^{-1} in FT-IR spectrum and 2974, 2942 cm^{-1} in FT-Raman spectrum. The calculated wavenumbers at 2997 and 2942 cm^{-1} have shown good agreement with observed bands. The symmetric stretching mode calculated at 2899 cm^{-1}, this vibration show good correlation with observed wavenumbers at 2844cm^{-1}/FT-IR and 2838 cm^{-}1/FT-Raman spectrum, respectively.

For methyl group, the symmetrical bending occurs near 1375 cm^{-1} and the asymmetrical bending vibration near 1450 cm^{-1} [42]. In the present study, asymmetric bending vibration observed at 1465, 1446 cm^{-1} in FT-IR spectrum and 1451 cm^{-1} in FT-Raman spectrum, these are in line with calculated wavenumbers at 1462, 1454 and 1447 cm^{-1}. Furthermore, symmetrical bending vibration observed as a weak band at 1342 and 1328 cm^{-1} in FT-IR and FT-Raman respectively, these wavenumbers show good agreement with calculated wavenumber at 1354 cm^{-1}.

C=O and C–O Vibration

The C=O stretching vibrations generally expected in the region of 1715–1600 cm^{-1}, it is moderately active in Raman and intense in IR [43]. In the present case the stretching mode of C=O is assigned at 1740 and 1689 cm^{-1} in FT-IR spectrum and 1733 cm^{-1} in FT-Raman spectrum. These wavenumbers computed at 1756 and 1753 cm^{-1}. The deformation vibration of carbonyl group observed at 715 cm^{-1} in FT-Raman spectrum, which shows good accordance with theoretical wavenumber at 723 cm^{-1}.

The C–O stretching vibrations usually occur in the region 1260–1000 cm^{-1} [43]. Sharp bands observed at 1028, 974 and 838 cm^{-1} in FT-IR spectrum and 1175, 1029, 865 cm^{-1} in FT-Raman spectrum are assigned for C–O stretching vibration. These vibrations theoretically calculated at 840, 865, 991, 1028, 1178 and 1239 cm^{-1} and shows good agreement with experimental wavenumbers. Deformation of C–O vibrations theoretically recorded at 684, 900 and 1098 cm^{-1}.

C–C and C–Cl Vibration

The carbon–carbon stretching modes of aromatic compounds generally appeared in the region of 1650-1200 cm^{-1} [44]. Most of the ring modes are altered by the substitution to aromatic ring. Hence, bands with variable intensity are observed [45]. In the present investigation, the bands observed at 1621, 1588, 1505, 1129 cm^{-1} in FT-IR and 1622 cm^{-1} in FT-Raman are assigned to C–C stretching vibration of the DTTP molecule and the calculated wavenumber show excellent correlation with observed value at 1616, 1577, 1484, 1423 and 1111 cm^{-1}. The C–C–C in-plane-bending vibration theoretically predicted at 908, 772 and 546 cm^{-1} by B3LYP method.

In pyrimidine ring, the stretching vibration of ν(C–C) has been calculated at 1066 and 1098 $cm^{-1.}$ These bands observed in FT-IR spectrum at 1097 cm^{-1}. The experimental wavenumber is in agreement with those in the calculated wavenumbers.

The stretching vibration for C–Cl bond observed as a strong band in the region 760-505 cm^{-1}[46]. In the present study, the C–Cl stretching band for the title compound is observed at665 cm^{-1} in FT-IR spectrum and 648 cm^{-1} in FT-Raman, the corresponding theoretical wavenumber shows good agreement with recorded wavenumbers and is calculated at 659 cm^{-1}.

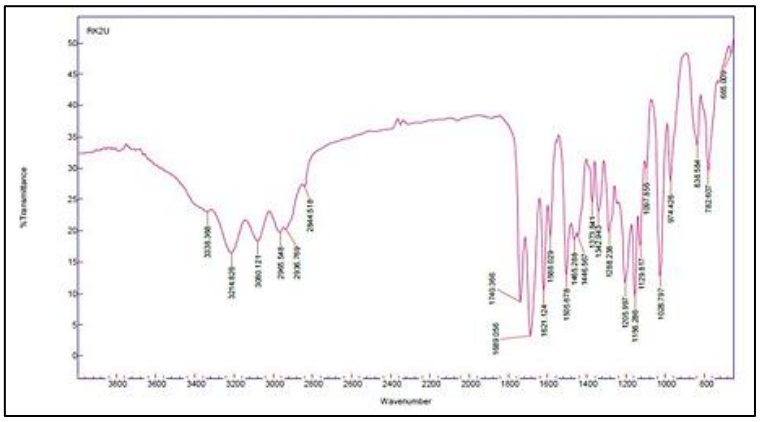

Figure 7: The FT-IR Spectrum of ECMC

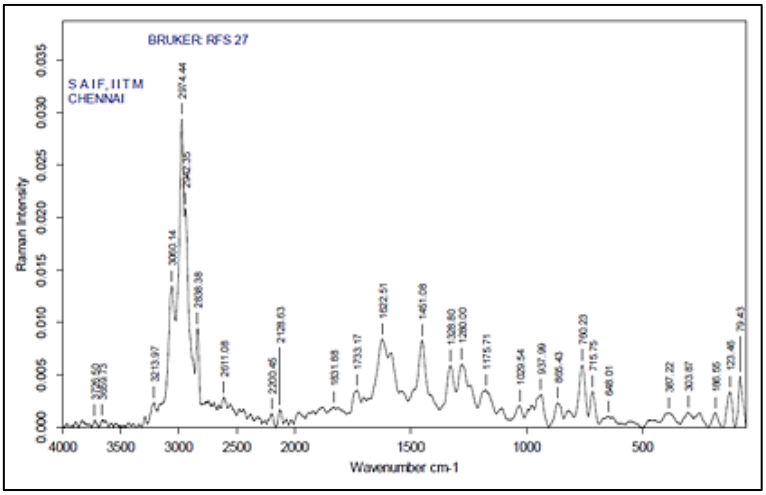

Figure 8: FT-Raman spectrum of ECMC

Table 6: The experimental and theoretical vibrational assignments of ECMC along with PED distributions

Mode no.	Calculated wavenumber (cm^{-1})		Observed wavenumber (cm^{-1})		Intensity		Assignments[d]
	Unscaled	Scaled	FT-IR	FT-Raman	IR	Raman	PED≥10%
1	3622	3484	3338 w		2.98	6.08	νN29H12(99)+νN30H14(99)
2	3619	3482	3214 w	3213 w	15.99	1.51	νN29H12(99)+νN30H14(99)
3	3229	3106			1.62	9.44	νC3H7(99)+ νC4H35(99)
4	3226	3103			0.2	4.08	νC16H17(99)+ νC16H33(100)
5	3209	3088	3080		0.92	4.78	νC3H7(99)+ νC4H35(99)

			w				
6	3193	3072		3060 w	1.05	5.23	νC6H8(99)
7	3149	3029			5.32	11.56	νC37H38(90)
8	3142	3023			6.57	1.32	νC20H25(97)+ νC20H26(99)+ νC21H22(98)+ νC21H23(99)
9	3138	3018			1.03	6.62	νC16H17(99)+ νC16H33(100)
10	3133	3014			4.59	7.83	νC21H22(98)+ νC21H23(99)+ νC21H24(97)
11	3115	2997		2974s	0.52	6.49	νC20H25(97)+ νC20H26(99)+ νC21H22(98)+ νC21H23(99)
12	3114	2996			1.87	6.4	νC9H18(99)
13	3084	2967	2965 w		1.11	6.16	νC10H32(99)
14	3074	2957			9.01	4.94	νC37H39(95)+ νC37H40(95)
15	3074	2957			2.26	6.29	νC20H25(97)+ νC20H26(99)
16	3058	2942	2936 w	2942 w	2.69	11.42	νC21H22(98)+ νC21H23(99)+ νC21H24(97)
17	3013	2899	2844vw	2838 w	12.73	12.71	νC37H39(95)+ νC37H40(95)
18	1825	1756	1740s	1733 w	100	3.48	νO31C11(73)
19	1822	1753	1689s		56.23	0.66	νO28C19(84)
20	1680	1616	1621s	1622 w	1.95	8.29	νC3C2(51)+ νC3C4(54)+ νC6C1(39)+ νC5C6(50)
21	1639	1577	1588 w		2.1	8.84	νC3C2(51)+ νC2C1(51)+ νC4C5(52)
22	1542	1484	1505 w		51.35	0.54	νC2C1(51)+βH7C3C2(54)+ βH8C6C1(45)
23	1530	1472			0.9	0.57	βH25C20H26(83)+ βH22C21H23(79)+ ΓC20H25C21H26(73)
24	1520	1462	1465vw		11.52	4.28	βH39C37H40(83)
25	1511	1454		1451 w	0.49	8.17	βH25C20H26(83)+ βH22C21H23(79)
26	1504	1447	1446vw		1.15	11.73	βH38C37H40(78)
27	1502	1445			1.21	9.36	βH23C21H24(80)+ ΓC21H24C20H22(64)
28	1489	1432			4.64	4.35	ΓC37H39H40H38(68)
29	1479	1423			10.33	1.01	νC3C4(54)+ νC6C1(39)+ βH35C4C3(33)
30	1472	1416			7.56	2.59	βH17C16H33(72)
31	1462	1407			12.11	2.14	βH14N30C13(56)
32	1452	1397			18.71	2.48	νN29C11(42)+ νN30C11(38)+ βH12N29C11(62)+ ΓC9C1C10H18(61)
33	1440	1385			3.25	4.33	ΓC20H25C21H26(73)+ ΓC21H22H23H24(83)
34	1417	1363	1373 w		3.85	0.98	νN30C11(38)+ βH12N29C11(62)+ βN29C11O31(49)
35	1407	1354	1342 w	1328 w	1.97	0.19	ΓC20H25C21H26(73)+ ΓC21H22H23H24(83)
36	1366	1314			19.17	1.83	βH32C10C19(40)
37	1360	1308			11.28	0.91	νC3C2(51)+ νC2C1(51)+ νC4C5(52)+ νC5C6(50)
38	1348	1297	1288 w	1280 w	1.17	1.63	βH18C9C1(44)+ ΓC10C9C19H32(56)
39	1329	1279			8.56	0.79	ΓH17C16C13C10(25)+ ΓH33C16C13C10(42)
40	1319	1269			17.45	9.12	νC3C4(54)+ νO36C5(32)
41	1304	1255			14.72	1.45	ΓC9C1C10H18(61)+ ΓC10C9C19H32(56)
42	1299	1250			0.28	6.61	βH25C20C21(93)
43	1288	1239			5.04	6.53	νO15C2(12)+ βH7C3C2(54)+ βH35C4C3(33)+ βH8C6C1(45)
44	1284	1236			39.28	2.38	ΓC9C1C10H18(61)
45	1254	1207	1205s		17	5.44	βH17C16C13(44)+ ΓC10C9C19H32(56)
46	1225	1178		1175 w	14.84	1.33	νO27C19(41)+ βH8C6C1(45)+ βH17C16C13(44)
47	1217	1171			46.52	3.54	νO27C19(41)+ βH32C10C19(40)+ βH17C16C13(44)
48	1214	1168	1156s		2.69	2.94	βH39C37O36(74)+ βH39C37H40(83)+

							ΓC37H38O36H39(69)
49	1184	1139			1.17	1.18	βH22C21C20(56)+ ΓC20C21O27H25(92)+ Γ C21H24C20H22(64)
50	1183	1138			4.29	2.38	νN30C13(27)+ βH8C6C1(45)+ βH18C9C1(44)
51	1180	1135			23.45	1.32	βH7C3C2(54)
52	1179	1134			0.12	2.89	βH39C37O36(74)+ ΓC37H38O36H39(69)
53	1154	1111	1129 w		14.76	3.98	νC3C4(54)+ νN30C13(27)+ βH35C4C3(33)
54	1141	1098	1097 w		1.35	4.85	νC21C20(62)+ βH22C21C20(56)+ βC21C20O27(67)+ Γ C21H24C20H22(64)
55	1127	1084			6.61	1.44	νC16C13(15)
56	1109	1066			11.45	3.51	νN29C9(29)+ νC10C9(22)
57	1079	1038			17.17	0.6	νC5C6(50)+ νO36C37(55)
58	1068	1028	1028s	1029 w	12.18	5.76	νC10C9(22)+ νO27C20(72)
59	1050	1010			7.7	3.14	νC21C20(62)+ νO27C20(72)
60	1030	991			34.55	1.35	νO15C13(30)+ τH33C16C13C10(42)
61	1010	972	974s		0.13	1.81	νO27C19(41)+ νC21C20(62)+ νC19C10(18)
62	971	934		937w	2.98	5.52	νN29C11(42)+ νN30C11(38)
63	944	908			2.41	7.38	νC4C5(52)+ νC5C6(50)+ βC4C5C6(27)
64	936	900			0.31	1.28	τH7C3C2O15(87)+ τH35C4C5O36(82)
65	899	865		865w	3.08	2.77	νO15C13(30)+ Γ C10C1N29C9(16)
66	894	860			4.64	8.09	νO27C20(72)+ Γ C6C1C5H8(74)
67	885	852			6.94	1.49	Γ C6C1C5H8(74)
68	873	840	838w		2.69	8.52	νO27C20(72)
69	848	816			1.86	0.63	βO27C19O28(45)
70	827	796			6.96	1.43	τH7C3C2O15(87)+ τH35C4C5O36(82)
71	813	783	782w		0.17	0.22	βH25C20C21(93)+ βH22C21C20(56)+ Γ C20C21O27H25(92)+ Γ C21H24C20H22(64)
72	802	772			5.71	1.89	βC2C1C9(14)
73	782	753		760w	8.48	13.79	βC1C9N29(14)+ Γ O31N29N30C11(81)
74	758	730			8.59	5.71	νCl34C16(57)+ Γ O31N29N30C11(81)
75	752	723		715w	4.05	17.81	νCl34C16(57)+ Γ O31N29N30C11(81)
76	728	700			0.95	7.97	Γ C3C1O15C2(66)
77	711	684			2.96	5.91	νN29C11(42)+ Γ C3C1O15C2(66)
78	685	659	665w	648w	2.17	2.4	νCl34C16(57)+ Γ O28C10O27C19(26)
79	665	640			10.55	3.45	βN29C11N30(16)
80	636	611			0.62	9.13	Γ O36C4C6C5(35)
81	620	596			2.92	1.37	βC2O15C13(25)+ Γ O36C4C6C5(35)
82	592	570			20.89	4.15	Γ N29C9C11H12(55)+ τH14N30C11N29(90)
83	567	546			4.31	3.11	βC5C6C1(14)
84	558	537			7.36	2.41	Γ N29C9C11H12(55)+ τH14N30C11N29(90)
85	554	533			5.82	5.41	Γ N29C9C11H12(55)+ τH14N30C11N29(90)
86	546	525			4.56	5.58	βN29C11O31(49)+ Γ N29C9C11H12(55)
87	499	480			3.44	3.35	τH14N30C11N29(90)
88	476	458			0.81	2.83	τC4C5C6C1(13)+ τC2C1C6C5(44)+ Γ C3C1O15C2(66)
89	441	425			0.16	5.59	βC4C5C6(27)+ βC37O36C5(26)
90	418	402			1.38	1.41	βN29C11O31(49)+ βC21C20O27(67)+ βC9N29C11(13)
91	409	394		387w	0.52	5.91	ΓO15C2N30C13(26)+ τC6C1C9C10(49)
92	393	378			0.03	5.41	βC21C20O27(67)+ τC2C1C6C5(44)+ Γ C3C1O15C2(66)
93	377	363			1.14	2.58	βO27C19O28(45)+ βC21C20O27(67)
94	328	315		303w	2.11	11.88	βO27C19O28(45)+ βO27C19C10(14)+ βC20O27C19(26)
95	307	296			0.6	10.38	βC16C13O15(38)+ βC20O27C19(26)
96	294	282			0.09	7.73	βC37O36C5(26)+ Γ N29C9C11C1(17)
97	275	265			0.57	1.57	τH23C21C20O27(73)
98	266	256			0.44	13.85	τH23C21C20O27(73)+ τH40C37O36C5(75)+ Γ O15C2N30C13(26)
99	252	242			0.2	13.25	βC16C13O15(38)+ τH40C37O36C5(75)
100	245	235			0.05	2.9	ΓH40C37O36C5(75)
101	209	201			0.36	5.46	βC9C10C19(16)+ βC13C16C34(27)
102	191	184		186w	0.46	7.17	τC9N29N30C11(25)
103	181	174			0.06	1.11	βC6C1C9(12)+ βC4C5O36(26)

104	158	152			0.66	4.54	τC20O27C19C10(67)+ τC19C10C13N30(48)
105	142	137			0.49	1.74	τC1C9C2O15(30)+ τN29C11C13N30(27)+ τC20O27C19C10(67)
							+ ΓC13N30O15C16(28)
106	134	129		123w	0.12	9.5	βC13C16C34(27)+ τC20O27C19C10(67)+ τC10C13C16C34(71)
							+ ΓC13N30O15C16(28)
107	86	83			0.22	4.81	τC20O27C19C10(67)
108	83	80			0.27	17.31	τC6C5O36C37(69)
109	78	75		79w	0.1	66.22	τC1C9C2O15(30)+ τC9N29N30C11(25)+ τN29C11C13N30(27)

ν: Stretching, δ: in-plane-bending, Γ: out-of-plane bending, vw: very weak, w: weak, m: medium, s: strong, vs: very strong,
[a]Scaling factor: 0.9608, [b]Relative IR absorption intensities normalized with highest peak absorption equal to 100,
[c]Relative Raman intensities calculated by Equation and normalized to 100.
[d]Potential energy distribution calculated at B3LYP/6-311++G(d,p) level.

CONCLUSION

In the present investigation, a highly functionalized dihydropyrimidine ECMC was synthesised by Biginelli condensation reaction. The structural identification of the synthesized compound is confirmed by FT-IR, FT-Raman, UV and NMR spectral analysis. The calculated fundamental wavenumbers were compared with experimental wavenumbers and it shows very good agreement with each other. The electronic absorption spectra reveals that n-π* and π-π* interaction takes place in the molecule, which is confirmed by FMO analysis.The major stabilization energy is also transferred from nonbonding orbital O_{27} to $\pi^*C_{19}–O_{28}$ resulting 207.44 kJ/mol. From the results of NLO studies, the ECMC compound has shown nonlinear optical activity, which is nine times greater that the reference molecule Urea. Hence, the synthesized compound is a good candidate for nonlinear optical studies.

REFERENCE

[1] C Kurumurthy; RP Sambasiva; SB Veera; KG Santhosh; RP Shanthan; B Narsaiah LR Velatooru; R Pamanji; RJ Venkateswara. *Eur J Med Chem.* **2011**, 46, 3462-3468.
[2] BA El-Gazzar; HN Hafez. *Bioorg Med Chem Lett.* **2009**, 19, 3392-3397.
[3] JM Quintela; CPeinador; L Botana; M Estevez; C Riguera. *Bioorg Med Chem.* **1997**, 5, 1543-1553.
[4] S Furuya; T Ohtaki. *Chem Abstr.* **1994,** 121, 205395.
[5] MF Hasan; AM Madkour; I Salem; JMA Rahman; EAZ Mohammed. *Heterocycles.* **1994,** 38, 57-69.
[6] Jdavoll; J Clarke; EF Elslager; Folate. *J Med Chem.* **1972**, 15, 837-839.
[7] AD Broom; JL Shim; GL Anderson. *J Org Chem.* **1976**, 41, 1095-1099.
[8] EM Grivsky; S Lee; CW Sigel; DS Duch; CA Nichol. *J Med Chem.* **1980**, 23, 327-329.
[9] RS Kanth; VG Reddy; HK Kishore; SP Rao; B Narsaiah; NS Murthy. *Eur J Med Chem.* **2006**, 41, 1011-1016.
[10] G Bereket; C Ogretir; M Yaman; E Hur. *J Mol Struct (THEOCHEM).* **2003,** 625, 31-38.
[11] MS Masoud; MK Awad; MA Shaker; MMT El-tahawy. *Corros Sci.* **2010,** 52, 2387-2396.
[12] EV Verbitskiy; EM Cheprakova; JO Subbotina. *Dyes Pigment*. **2014**, 100, 201-214.
[13] EH Anouar. *Antioxidants*. **2014**, 3(2), 309-322.
[14] A Amic; ZMarkovic; JM DimitricMarkovic; V Stepanic; B Lucic; Damic. *Food Chem.* **2014,** 152, 578-585.
[15] MH Jamroz. Vibrational Energy Distribution Analysis: VEDA4 program, Warsaw, Poland, **2004**.
[16] A Dhandapani; S Manivarman; SSubashchandrabose; Bgunasekaran. *Acta Cryst.* **2015**, E71, 117-118.
[17] JP Foster; F Weinhold. *J Am Chem Soc.* **1980**, 102, 7211-7218.
[18] J Chocholousova; VV Spirko; P Hobza. *Phys Chem Phys.* **2004**, 6, 37-41.
[19] ED Glendening, AE Reed, JE Carpenter, F Weinhold. NBO Version 3.1, TCI, University of Wisconsin, Madison, **1998**.
[20] JS Murray; K Sen; Molecular Electrostatic Potentials, Concepts and Applications, *Elsevier*. Amesterdam, **1996.**
[21] FE TaibHeakal; SK Attia; SA Rizk; MA Abou Essa; AE Elkholy. *J Mol Struct.* **2017**, 1147, 714-724.
[22] M Habibi; SA Beyramabadi; S Allameh; M Khashi; A Morsali; M Pordel; MK Chenarboo. *J Mol Struct.* **2017**, 1143, 424-430.
[23] N Sinha; O Prasad; V Naryan; SR Shukla. *J Mol Simul.* **2011**, 37, 153-163.
[24] S Muthu; JU Maheswari. *Spectrochim Acta Part A.* **2012,** 92, 154-163.
[25] K Govindarasu; E Kavitha. *Spectrochim Acta Part A: Mol Bimol Spectros.* **2014**, 122, 130-141.

[26] K Govindarasu; E Kavitha; N Sundaraganesan; *Spectrochim Acta Part A: Mol Biomol Spectros.* **2014**, 133, 417-431.
[27] K Chaitanya. *Spectrochim Acta Part A.* **2012,** 86, 159-173.
[28] S Sebastian; N Sundaraganesan, B Karthikeiyan, V Srinivasan. *Spectrochim Acta Part A.* **2011,** 78, 590-600.
[29] M Raja; RR Muhamed; S Muthu; M Suresh. *J Mol Struct.* **2017**, 1141, 284-298.
[30] K Govindarasu; E Kavitha; N Sundaraganesan. *Spectrochim Acta Part A: Mol Biomol Spectros.* **2014,** 133, 417-431.
[31] MS Almutairi; S Xavier; M Sathish; HA Ghabbour; S Sebastian; S Periandy; RI Al-Wabli; MI Attia. *J Mol Struct.* **2017**, 1133, 199-210.
[32] S Sebastian; N Sundaraganesan. *Spectrochim Acta Part A.* **2010,** 75, 941-952.
[33] G Socrates. Infrared and Raman Characteristic Group Frequencies, Tables and Charts, third ed., Wiley, Chichester, **2001**.
[34] YR Sharma. Elementary Organic Spectroscopy, Principles and Chemical Applications, S. Chande and Company Ltd., New Delhi, **1994**.
[35] MH Jamroz; J Dobrowolski; RCz Brzozowksi. *J Mol Struct.* **2006**, 787, 172-183.
[36] A Altun; K Golcuk; M Kumru. *J Mol Struc (Theochem).* **2003**, 637, 155-169.
[37] FR Dollish, WG Fateley, FF Bentely. Characteristic Raman Frequencies on Organic Compounds, Willey, New York, **1997**.
[38] BV Reddy; G Ramana Rao. *Vibr Spectr.* **1994**, 6, 231-250.
[39] B Smith. Infrared Spectral Interpretation a Systematic Approach, CRP Press, Washington, DC, **1999**.
[40] NB Colthup, LH Daly, SE Wiberly. Introduction to Infrared and Raman Spectros., Academic Press, New York, **1990**.
[41] XH Li; TW Li; WWei Ju. *Spectrochim Acta Part A; Mol Bimol Spectros.* **2014**, 118, 503-509.
[42] NPGRoeges. A Guide to the Complete Interpretation of Infrared Spectra of Organic Compounds, Wiley, New York, **1994**.
[43] G Varsanyi. Vibrational Spectra of Benzene Derivatives, Academic Press, New York, **1969**.
[44] V Arjunan; S Sakiladevi; MK Marchewka; S Mohan. *Spectrochim Acta Part A.* **2013**, 109, 79-89.
[45] LJ Bellamy. The Infrared Spectra of Complex Molecules, Wiley, Newyork, **1959**.
[46] T Chithambarathanu; V Umayorubagan; V Krishnakumar. *Ind J Pure Appl Phys.* **2002,** 40, 72-74.